Proceedings of HT/FED'04
2004 Heat Transfer/Fluids Engineering Summer Conference
July 11-15, 2004, Charlotte, North Carolina, USA

HT-FED2004-56790

AN UNCERTAINTY ANALYSIS OF A NIST HYDROCARBON LIQUID FLOW CALIBRATION FACILITY

T. T. Yeh, P. I. Espina, G. E. Mattingly, and N. R. Briggs
National Institute of Standards and Technology
100 Bureau Drive, Gaithersburg, MD 20899-8361, USA

Jesús Aguilera
Centro Nacional de Metrología
Querétaro, Qro., México

ABSTRACT

This paper presents the uncertainty characterization of NIST's new hydrocarbon liquid flow calibrator (HLFC). This facility uses a passive piston prover technique where fluid is driven by pumps while the measuring piston is passively stroked through the calibration interval. This facility is typically operated using MIL-C-7024C fluid,[£] but using a variety of other fluids offers a wider range of measurements. The range of flows for this facility is 0.19 to 5.7 liters per minute – lpm (0.05 to 1.5 gallons per minute – gpm). Over this range, the expanded uncertainty claim for this facility is ±0.01%, at 95% confidence level. The uncertainty of a dual-turbine meter tested in the system is also reported. In addition, NIST is working to incorporate additional piston provers so that the flow for hydrocarbon liquids calibration service will reach 760 lpm (200 gpm).

INTRODUCTION

In flow metrology there is no "standard" device, physical artifact, or thermodynamic definition equivalent to standards used to specify other measurement quantities such as length, mass or temperature. Instead, flow measurements are derived from fundamental measurements such as mass, length, time, and temperature, typically by accounting for the transfer of a known mass or volume of fluid over a measured time interval. Such flow metrology facilities are known as "primary flow standards", and by definition, they are facilities capable of determining flow, at specified uncertainty levels, without being calibrated for the unit of flow being realized.

Operators of primary flow standards seek to validate the claimed uncertainties of their standards by establishing and maintaining the traceability of calibration results to the SI. One complete way to establish traceability involves the use of proficiency testing techniques, which quantify the traceability of a facility's results using a set of flow standards maintained by a National Metrology Institute (NMI) [1]. Proficiency testing is considered "complete" because it quantifies a facility's capabilities in relation to a referenced standard in actual flow meter calibration conditions, which include all of the components of the facility as well as the dynamical aspects of a calibration.

Alternatively, establishing traceability can also be done through a process of assessing the individual components of a facility, analyzing their respective contributions to the calibration process, and estimating the dynamical aspects of a calibration. This alternative procedure is generally less attractive than proficiency testing because some components can be overlooked (*e.g.,* operator effects, software and computation errors). Despite these limitations, an extensive component analysis of NIST's HLFC was performed. In the following sections, a description of the assessment of NIST's HLFC using the component analysis method is given. Subsequent to this study, NIST intends to conduct proficiency testing or Key Comparisons among other NMIs to confirm the uncertainty results obtained through this analysis.

NOMENCLATURE

$\vec{A}$ ..... vectorial area element
D ..... piston diameter
E ..... spatial variation of the fluid temperature
K_E ..... encoder constant (pulses/cm)
L ..... piston stroke length
M ..... mass
N_E ..... encoder pulses
Q ..... average volume flow rate

[£] Also know as Stoddard solvent – a surrogate liquid for JP-4 and JP-5 jet fuels.

T .....temperature
$\vec{U}$ .....vectorial velocity
U_{CV} .....average fluid velocity in the connecting volume
V .....volume
d .....shaft diameter
d_{CV} .....connecting pipe diameter
$c_{x_i,y}$ .....dimensionless sensitivity coefficient of x_i and y
c_P .....specific heat capacity of the fluid
l_{CV} .....connecting pipe length
r_{ij} .....cross correlation coefficient between variables x_i and x_j
$u(x_i)$ .....standard uncertainty of the variable x_i
u_A, u_B .....types of uncertainty
u_{x_i} .....dimensionless uncertainty of x_i
$u_c(y)$ .....combined standard uncertainty of y
t .....time
x .....distance measured from the piston
x_i ..... i -th variable
x_{MUT} .....MUT position
y .....measurement quantity
$\Delta( )$ .....change of ( )
ΔH .....total heat transfer to the fluid element in the connecting volume
$\sum( )$ .....summation of ( )
α .....thermal expansion coefficient for the fluid density
α_s .....linear expansion coefficient of the pipe
α_E .....linear expansion coefficient of the encoder
ρ .....fluid density
σ .....standard deviation
$\overline{\sigma}$ .....standard deviation of the mean

subscripts

c .....calibration
CP .....connecting pipe
CV .....connecting volume
ER .....encoder at reference temperature
F .....fluid
max .....maximum
MUT .....meter under test
I, II, III ...three parts of fluid
L .....fluid leak
P .....piston
r .....residence
i, f .....initial and final
j ..... j -th fluid element
0 .....reference or mean condition

PISTON PROVER CALIBRATION SYSTEMS

Piston prover systems have long been accepted as primary flow calibrators for both gas and liquid flow meters [2, 3]. In its most basic form, the piston prover system consists of a circular cylinder of known internal diameter, which encompasses a sealed piston. This piston strokes through measured lengths, at a constant speed, to produce a volumetric flow. Conservation of mass principles, prover volumetric flow rates, and fluid density measurements govern the calculation of flow through the meters under test (MUT).

Two types of piston arrangements are generally used in these systems. An *active* piston can both drive and measure a volumetric flow out of the cylinder (*e.g.,* a hypodermic needle), while a *passive* piston operates via pumped fluid, which drives the piston through the calibration stroke to determine the volumetric flow rate. The NIST HLFC employs a passive piston.

Both active and passive piston provers begin operation essentially after flow through the cylinder, the pipeline connecting the MUT to the cylinder, and the MUT, all reach steady state conditions. An analysis of this calibration situation is given below, accompanied by an uncertainty analysis of NIST's HLFC.

DESCRIPTION OF THE NIST FACILITY

The NIST's HLFC facility was manufactured by Flow Dynamics Inc, in Scottsdale, AZ.* The analysis that follows applies only to the smallest of the three piston-cylinder systems that will ultimately constitute NIST's Hydrocarbon Liquid Flow Measurement Standard. These three systems are very similar in design and in operating principle, and a component analysis of the two larger cylinders will follow in a future publication. The complete facility will enable NIST to calibrate a MUT in flows as large as 760 lpm. Table 1 shows the nominal sizes of the three calibrators.

The small HLFC system analyzed below will be used for flows between 0.19 lpm and 5.7 lpm. Figure 1 shows a photo of the calibrator and Figure 2 provides its schematic diagram. The system uses two pumps operating in a bi-directional mode, which allows the pumped liquid to move the piston back and forth. To attain unidirectional flow through the MUT, two three-way valves are applied to the bi-directional system shown in Figure 2. To allow operation in varied flow conditions, a computer-controlled stepping-motor drives both pumps. The size of the small pump is about one tenth the larger one. At lower flow conditions, the flow from the large pump is redirected to the reservoir tank.

* Certain commercial equipment, instruments, or materials are identified in this paper to foster understanding. Such identification does not imply recommendation or endorsement by the National Institute of Standards and Technology, nor does it imply that the materials or equipment identified are necessarily the best available for the purpose.

Table 1. Nominal Characteristics of NIST's Hydrocarbon Liquid Flow Calibrators.

	Small Calibrator	Medium Calibrator	Large Calibrator
D , [cm]	7.62	15.24	30.48
d , [cm]	2.54	2.54	2.54
L , [cm]	55	110	140
L_c , [cm]	14 – 37.4**	n/a	n/a
V_c , [cc]	567 – 1515**	n/a	n/a
t_c , [sec]	15 – 180**	n/a	n/a
u_C , [%]	0.005	n/a	n/a
$u_{k=2}$, [%]	0.01	n/a	n/a
Q , [lpm]	0.19 – 5.7	4.5 – 125	100 – 760

Figure 1. Photograph of the small Liquid Flow Calibrator.

PRINCIPLE OF OPERATION

The operation of the four-way diverter valve is demonstrated schematically in Figures 2 and 3. The calibration interval begins as soon as flow conditions reach steady state once the piston accelerates to constant velocity (shortly after the piston begins travel in one direction). The meter calibration stroke interval ends before the piston reaches the transition phase. During the transition period when the piston changes direction, both of the three-way valves are set so that all three ports are open, thus preventing any hydraulic ram effects. The average volumetric flow rate exiting the prover is given by the volume displaced by the piston divided by the duration of the calibration interval.

** Specific values are selected to conform to results of this uncertainty analyses.

Steady state temperature conditions are achieved by cycling the piston back and forth at the intended calibration flow, which promotes the mixing of the fluid. Thermal equilibrium is further enhanced by forcing the calibration fluid through an outer cylindrical jacket that encloses the cylinder and piston. The liquid flow from the pumps is directed into this outer jacket before entering the four-way diverter valve. The benefits of using this outer jacket include: (a) better temperature uniformity among different parts of the fluid and the prover, and (b) pressure balance inside and outside of the prover, preventing a pressure gradient from affecting the size of the piston diameter. A chilled water heat exchanger controlled by a feedback temperature sensor, is used to remove heat from the fluid added by friction and the pumps. The calibrator uses twelve temperature sensors to determine fluid properties throughout the flow loop. The locations are indicated in Figure 2. Furthermore, the calibrator is located in a temperature-controlled room where the air temperature is maintained at $22.2 \pm 0.5\ ^{o}C$.

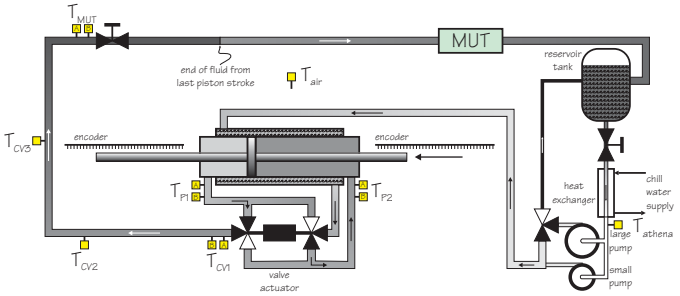

Figure 2. Sketch of the calibrator with piston stroking left.

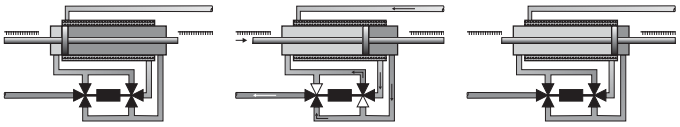

Figure 3. Sketch of piston and three-way valves reversing piston directions: *left figure* – transition from left to right piston stroke, *center figure* – piston stroking right, and *right figure* – transition from right to left piston stroke.

This calibrator measures the volumetric flow of fluid through the MUT from the fluid discharged by the piston-cylinder assembly over a precisely measured time period. Since leaks or temperature and pressure changes may cause the total mass in the pipe that connects the piston-cylinder assembly to the MUT to change during the calibration, the flow through this meter may differ from the flow exiting the cylinder. If no leaks are found, if corrections for temperature and pressure effects have been made, and if the fluid volume change in the connecting pipe is accounted for, the volumetric flow of the calibration can be obtained. Most previous prover analyses do not include corrections for fluid mass change in the connecting

volume and fluid density is assumed constant during the calibration. However, the connecting volume effect could contribute a significant error in the volume flow rate determination.

Different methods can be used in accounting for the connecting volume effect. The most common correction technique uses the mass conservation method. In addition to the mass conservation method, a volume balance method is included in the analysis provided here.

Mass Conservation Method: The operational principle of the piston prover is the conservation of mass. The general equation for the conservation of mass is:

$$\frac{\partial}{\partial t}\int_V \rho\, dV + \int_A \rho \vec{U}\cdot d\vec{A} = 0 \tag{1}$$

where ρ is the fluid density; $\partial / \partial t$ is the partial derivative with respect to time; V is a control volume used to assess the specified mass balance; and $\vec{U}$ is the vectorial velocity across the vectorial area element, $d\vec{A}$, of the control surface (surrounding the control volume) with the positive direction outward, such that the positive $\vec{U}\cdot d\vec{A}$ product denotes outflow. Equation (1) states that mass is neither created nor destroyed. For this system, that is, the initial fluid mass in the control volume, at the beginning of the calibration time interval equals the final fluid mass at the end of the calibration,

$$M_{Fi} = M_{Ff} \tag{2}$$

where the subscripts i and f denote the initial and final conditions. For a piston prover calibrator as shown in Figure 4, the initial fluid mass M_{Fi} is

$$M_{Fi} = M_{Pi} + M_{CVi} + M_{MUTi} \tag{3}$$

and the final fluid mass M_{Ff} is

$$M_{Ff} = M_{Pf} + M_{CVf} + M_{MUTf} + M_L \tag{4}$$

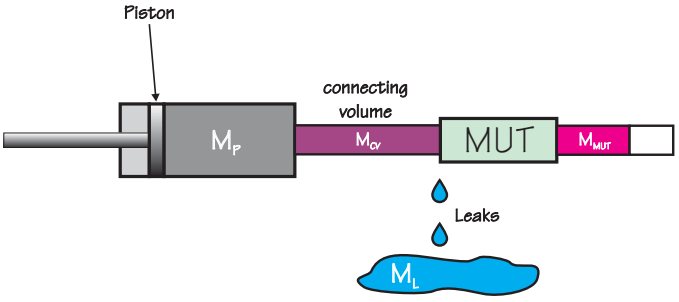

Figure 4. Mass conservation as applied to an incompressible piston system.

In (3) and (4), the subscripts P, CV, and MUT denote the piston, connecting volume, and MUT, respectively. M_L is any mass leaking from the system between the prover and MUT. The leakage is usually apparent and leaks are repaired before the calibrator can be used. Therefore, the leakage term M_L is hereafter assumed to be zero.

From (2) ~ (4), we have the mass of fluid passing through the MUT as:

$$\Delta M_{MUT} = M_{MUTf} - M_{MUTi} = \Delta M_P - \Delta M_{CV} \tag{5}$$

where

$$\Delta M_P = M_{Pi} - M_{Pf} = \int_{V_{Pi}} \rho\, dV - \int_{V_{Pf}} \rho\, dV \tag{6}$$

is the total mass displaced by the piston during the time period, t_c, and

$$\Delta M_{CV} = M_{CVf} - M_{CVi} \tag{7}$$

is the total mass difference in the connecting volume during the same period, t_c. When the fluid density in the piston is constant during the calibration time and equal to ρ_P, (6) simplifies to:

$$\Delta M_P = \int_{V_{Pi}} \rho\, dV - \int_{V_{Pf}} \rho\, dV = \rho_{Pi} V_{Pi} - \rho_{Pf} V_{Pf} = \rho_P\, \Delta V_P \tag{8}$$

where ΔV_P is the total volume displaced by the piston moving along the cylinder in the calibration in time, t_c.

CONNECTING VOLUME EFFECTS

In general, the fluid density is a function of pressure and temperature. However, in this liquid calibrator, the effect of the pressure variation is negligible, since the pressure is nearly constant throughout the system and the modulus of elasticity of the calibration liquid is large ($\approx 2\times10^9$ Pa). Therefore, in this analysis, the liquid density is assumed to be a function of the temperature only. Similarly, the structural length and volume of the connecting piping is assumed to be a function of temperature only (*i.e.,* no structural deformation in the pipe due to pressure). For a small temperature change, ΔT, the following linear relationships are assumed:

$$\begin{aligned} \rho &= \rho_0\left(1-\alpha\Delta T\right) \\ L &= L_0\left(1+\alpha_s\Delta T\right) \\ V &= V_0\left(1+3\alpha_s\Delta T\right) \end{aligned} \tag{9}$$

where α is the thermal expansion coefficient for the liquid density, and α_s is the linear expansion coefficient for the connecting pipe. Thus, any mass change in the connecting volume can be expressed as:

$$\begin{aligned}\Delta M_{CV} &= \Delta(\rho V)_{CV} \\ &= \rho_{CV}\Delta V_{CV} + V_{CV}\Delta\rho_{CV} \\ &= \rho_{CV}\left(V_{CV}\,3\alpha_s\Delta T_{CP}\right) - V_{CV}\left(\rho_{CV}\alpha\Delta T_{CV}\right) \\ &= \left(\rho_{CV}V_{CV}\right)\left(3\alpha_S\Delta T_{CP} - \alpha\Delta T_{CV}\right)\end{aligned} \tag{10}$$

where ρ_{CV} is the average fluid density in the connecting volume; V_{CV} is the average connecting volume; ΔT_{CP} is the temperature rise of the connecting pipe between the initial and final times for the calibration interval; and ΔT_{CV} is the temperature rise of the fluid in the connecting volume between the initial and final times.

Substituting (8) and (10) into (5), the fluid mass through the MUT in the calibration interval, t_c, becomes

$$\Delta M_{MUT} = \rho_P\Delta V_P - \left(\rho_{CV}V_{CV}\right)\left(3\alpha_s\Delta T_{CP} - \alpha\Delta T_{CV}\right) \tag{11}$$

Dividing (11) by the fluid density in the MUT, ρ_{MUT}, and the calibration interval, t_c, the average volume flow rate through the MUT, Q_{MUT}, becomes:

$$Q_{MUT} = \frac{\Delta M_{MUT}}{\rho_{MUT}\,t_c} = \frac{\rho_P\Delta V_P - \left(\rho_{CV}V_{CV}\right)\left(3\alpha_s\Delta T_{CP} - \alpha\Delta T_{CV}\right)}{\rho_{MUT}\,t_c} \tag{12}$$

From (9), the density ratios can be expressed as:

$$\frac{\rho_P}{\rho_{MUT}} = 1 - \alpha\Delta T_{P,MUT} \text{ and } \frac{\rho_{CV}}{\rho_{MUT}} = 1 - \alpha\Delta T_{CV,MUT} \tag{13}$$

where $\Delta T_{P,MUT}$ is the temperature difference between the fluid in the piston prover and the fluid in the MUT and $\Delta T_{CV,MUT}$ is the average temperature difference between the fluid in the connecting volume and that in the MUT. Substituting equation (13) into (12), the volume flow rate equation becomes:

$$Q_{MUT} = \frac{1}{t_c}\left[\begin{aligned}&\Delta V_P(1-\alpha\Delta T_{P,MUT}) - V_{CV}\left(3\alpha_S\Delta T_{CP} - \alpha\Delta T_{CV}\right) \\ &+\alpha\Delta T_{CV,MUT}\;V_{CV}\left(3\alpha_S\Delta T_{CP} - \alpha\Delta T_{CV}\right)\end{aligned}\right] \tag{14}$$

The last term in (14) is a second order expansion quantity which can be neglected based on a magnitude analysis. Hence, the final equation for volume flow rate becomes:

$$Q_{MUT} = \frac{1}{t_c}\left[\Delta V_P(1-\alpha\Delta T_{P,MUT}) + V_{CV}\left(\alpha\Delta T_{CV} - 3\alpha_S\Delta T_{CP}\right)\right] \tag{15}$$

From (15), it can be seen that the fluid density does not directly affect the calculation of the volumetric flow rate; however, any change in fluid density in the connecting volume is given by the terms $-\alpha\,\Delta T_{P,MUT}$ and $V_{CV}\alpha\,\Delta T_{CV}$. Thus the value of liquid density is only important if a mass flow, $\rho_{MUT}Q_{MUT}$, is needed.

Volume Balance Method: An alternate method for correcting fluid volume in the connecting volume is the volume balance method. For a given fluid, the change of its volume, ΔV_F, is given by the final fluid volume, V_{Ff}, minus the initial fluid volume, V_{Fi}, or,

$$\Delta V_F = V_{Ff} - V_{Fi} \tag{16}$$

Using Figure 5 as a reference, the initial fluid volume can be expressed as,

$$V_{Fi} = \left(V_P + V_{CV} + V_{MUT}\right)_i \tag{17}$$

while the final fluid volume is given by,

$$V_{Ff} = \left(V_P + V_{CV} + V_{MUT}\right)_f + V_L \tag{18}$$

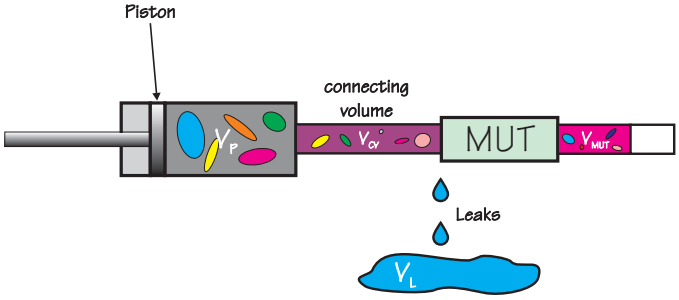

Figure 5. Balance of fluid quantities throughout the control volume. Different colors denote different fluid temperatures or different fluid densities.

In (17) and (18), V_{Pi} and V_{Pf} are the fluid volumes contained in the piston prover at the initial (start) and final (stop) times, respectively. Similarly, V_{CVi} and V_{CVf} are the fluid volumes contained within the connecting pipe at the initial and final times, respectively. V_{MUTi} and V_{MUTf} are the fluid volumes discharged through the MUT at the initial and final times, respectively, and V_L is the volume of any leaked fluid. As discussed above, the leakage V_L will be assumed to be zero and not considered further in this discussion.

Combining (16-18), we obtain an expression for the net fluid volume discharged through the meter,

$$\Delta V_{MUT} = V_{MUTf} - V_{MUTi} = \Delta V_F + \Delta V_P - \Delta V_{CV} \tag{19}$$

where, $\Delta V_P = V_{Pi} - V_{Pf}$ is the net fluid volume displaced by the piston, and $\Delta V_{CV} = V_{CVf} - V_{CVi}$ is the change of the connecting volume due to thermal expansion of the connecting pipe. Next, we shall discuss each of the volume change terms.

The volume change of the connecting volume due to the temperature change, ΔT_{CP} can be expressed as,

$$\Delta V_{CV} = V_{CV} 3\alpha_S \Delta T_{CP} \quad (20)$$

where, V_{CV} is the average connecting volume.

In contrast to ΔV_{CV}, the volume change of the fluid, ΔV_F is more difficult to estimate. As seen before, because the modulus of elasticity of the fluid is very large (2×10^9 Pa) and the working pressure is small in comparison (8×10^4 Pa), and fairly constant ($\Delta P < 80$ Pa), the density of the liquid can be assumed to be function of fluid temperature only. Thus, for a given mass of fluid, changes in fluid volume will only be due to changes in fluid temperature. For a small change of temperature ΔT, it can be shown that:

$$\rho = \rho_0(1-\alpha\Delta T),\ \Delta\rho = -\rho_0\alpha\Delta T \text{, and } V = V_0\alpha\Delta T \quad (21)$$

If the fluid volume is divided into small volume elements, V_j (see Figure 5), such that each small volume has constant fluid temperature, T_j, the volume change of each element can be expressed as,

$$\Delta V_j = V_j\alpha\Delta T_j = \alpha\,\Delta H_j/(\rho c_P) \quad (22)$$

where ΔH_j is the heat transferred to the j-th element of the fluid, and c_P is the specific heat capacity of the fluid. By summing over all elements, the total (or net) volume increase of the fluid is,

$$\Delta V_F = \sum\Delta V_j = (\alpha/\rho c_P)\sum\Delta H_j = (\alpha/\rho c_P)\Delta H \quad (23)$$

where ΔH is the total (or net) heat addition to the fluid in the connecting volume during the calibration time t_c.

From (23), it is worth noting that heat transfer between cold and hot pockets of fluids does not change the total volume of the fluid. Only net heat addition to the fluid will change the total fluid volume. Thus, if there is no net heat addition to the fluid, there will be no change in the fluid volume.

In our calibrator, an inevitable portion of the heat addition is due to viscous dissipation as the fluid moves through the pipe. The remainder heat contribution is due to heat transfer between the pipe and fluid. Thus, the net heat addition is normally a function of flow and the temperature difference between the calibrator and the ambient air. Insulating the connecting pipe can reduce the heat transfer between the room, thus reducing the amount of heat transfer between the pipe and fluid. Also, operating the calibrator at a steady, near-room temperature, will reduce this heat transfer. Equation (23) further shows that, large temperature coefficients, α, will lead to large volume increases, while large fluid densities, ρ, or specific heat capacities, c_P, will result in smaller volume increases.

According to the conservation of heat, the heat addition, ΔH, is related to the average temperature rise of the fluid as it moves through the connecting volume, $\Delta T_{H,CV}$, as:

$$\Delta H = \rho c_P \Delta V_P \Delta T_{H,CV} \quad (24)$$

Under normal operational conditions, the heat addition is a system characteristic which should be fairly constant.

By combining (23) and (24) and eliminating the heat addition, ΔH, the fluid volume change, ΔV_F, becomes:

$$\Delta V_F = \Delta V_P \alpha\,\Delta T_{H,CV} \quad (25)$$

This equation shows that the fluid volume increase depends only on the temperature rise, $\Delta T_{H,CV}$, and the thermal expansion coefficient of the fluid, α, but not on the fluid specific heat capacity.

By combining (19), (20) and (25) and dividing by the calibration time, t_c, we obtain the average fluid volume flowing through the MUT. That is,

$$Q_{MUT} = \frac{\Delta V_{MUT}}{t_c} = \frac{1}{t_c}\left[\Delta V_P(1+\alpha\,\Delta T_{H,CV}) - 3V_{CV}\alpha_S\Delta T_{CP}\right] \quad (26)$$

Once again, it is worth noting that the fluid density does not directly affect the volume flow calculation. Next, we will discuss how we determine the fluid temperature rise in the connecting volume during the calibration.

The fluid passing through the MUT is not exactly the same fluid that is being discharged from the prover. For the sake of discussion, the fluid that affects the average temperature rise can be divided into three parts: I, II and III. Figure 6 shows the sketch of the distribution of the three parts of fluids and the temperature variations as functions of time at MUT, T_{MUT}, and at piston, T_P. Part I fluid is the fluid found in the connecting volume at the time the calibration starts. During the calibration period, this fluid is pushed through the MUT. All of the fluid in Part II is displaced by the piston and passes through the MUT during the calibration period. The fluid in Part III is also displaced by the piston but does not reached the MUT before the calibration ends (*i.e.,* still in the connecting volume). The determination of the temperature rise for the fluid in part II is simple, while those for part I and III are more complex. The average temperature rise, $\Delta T_{H,CV}$ is thus the weighted average temperature rise of the three parts of fluid.

For each fluid element, its temperature rise is the difference of its temperatures at the initial and final times. To help illustrate this point, the fluid temperature at position x and time t is given as $T(x,t)$. Here, x is the distance measured from the piston, *i.e.,* $x=0$ at the piston and $x = x_{MUT}$ at the MUT. The temperature at two special locations, the MUT and the piston, (shown on Figure 6) are:

$$T_{MUT}(t) = T(x_{MUT},t) \text{ and } T_P(t) = T(0,t) \quad (27)$$

and the temperatures at two special times, the initial and final times, are:

$$T_i(x) = T(x,0) \text{ and } T_f(x) = T(x,t_c) \tag{28}$$

The position of a fluid element at time t, x, can be expressed by

$$x = x_0 + U_{CV} t \tag{29}$$

where x_0 is the initial position of the fluid, and $U_{CV} = 4Q_{MUT} / \pi d_{CV}^2$ is the average fluid velocity in the connecting volume. Here, d_{CV} is the inner diameter of the connecting pipe.

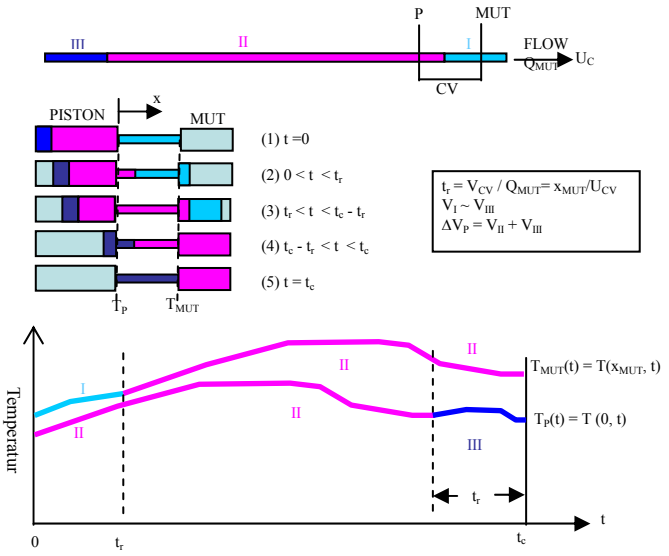

Figure 6. Sketch and estimation of the average temperature rise of fluid as it moves through the connecting volume. U_{CV} is the average flow velocity in the connecting volume. $T_{MUT}(t)$ and $T_P(t)$ are the temperature as functions of time at the MUT and at the prover, respectively.

As referred to Figure 6, we have the average temperature rise

$$\Delta T_{H,CV} = \frac{1}{t_c}\left(\int_0^{t_r} \Delta T_I \, dt + \int_{t_r}^{t_c} \Delta T_{II} \, dt + \int_{t_c - t_r}^{t_c} \Delta T_{III} \, dt \right) \tag{30}$$

where

$$\Delta T_I = T_{MUT}(t) - T(x_{MUT} - U_{CV} t, 0) \tag{31}$$

is the temperature rise of the fluid element I located at the MUT and time t;

$$\Delta T_{II} = T_{MUT}(t) - T_P(t - t_r) \tag{32}$$

is the temperature rise of the fluid element II; and

$$\Delta T_{III} = T(U_{CV}(t_c - t), t_c) - T_P(t) \tag{33}$$

is the temperature rise of the fluid element III located at the Piston and time t.

Inserting (31~33) into (30), we have

$$\begin{aligned}
\Delta T_{H,CV} &= \frac{1}{t_c}\left(\begin{array}{l} \int_0^{t_r} [T_{MUT}(t) - T(x_{MUT} - U_{CV} t, 0)]dt + \int_{t_r}^{t_c} [T_{MUT}(t) - T_P(t - t_r)]dt \\ + \int_{t_c - t_r}^{t_c} [T(U_{CV}(t_c - t), t_c) - T_P(t)]dt \end{array} \right) \\
&= \frac{1}{t_c}\left(\begin{array}{l} \int_0^{t_c} T_{MUT}(t)dt - \int_0^{t_c} T_P(t)dt \\ - \int_0^{t_r} T(x_{MUT} - U_{CV} t, 0)dt + \int_{t_c - t_r}^{t_c} T(U_{CV}(t_c - t), t_c)dt \end{array} \right) \\
&= T_{MUT,m} - T_{P,m} + \frac{1}{t_c}\left[\int_0^{x_{MUT}} T(x, t_c)\frac{dx}{U_{CV}} - \int_0^{x_{MUT}} T(x, 0)\frac{dx}{U_{CV}} \right] \\
&= -\Delta T_{P,MUT} + \frac{t_r}{t_c}\left(T_{CV,f} - T_{CV,i} \right) \\
&= -\Delta T_{P,MUT} + \frac{V_{CP}}{\Delta V_P}\Delta T_{CV}
\end{aligned} \tag{34}$$

Thus, when substituting (34) into (26), we obtain the average fluid volume flowing through the MUT as,

$$Q_{MUT} = \frac{1}{t_c}\left[\Delta V_P (1 - \alpha \Delta T_{P,MUT}) + V_{CV}(\alpha \Delta T_{CV} - 3\alpha_S \Delta T_{CP}) \right] \tag{35}$$

This equation is exactly (15), which was obtained from the mass conservation method.

UNCERTAINTY ANALYSIS

The uncertainty components of the NIST Hydrocarbon Liquid Flow Calibrator system are discussed below. As seen in (15), they include the uncertainty of the following elements:

(a) the displaced prover volume, ΔV_P,
(b) the thermal expansion coefficient for the liquid density, α,
(c) the linear thermal expansion coefficient for the piping, α_S,
(d) several induced temperature differences ($\Delta T_{P,MUT}$, ΔT_{CP}, ΔT_{CV}), and
(e) the connecting volume, V_{CV}.

Figure 7 shows a graphic representation of the uncertainty analysis for this system.

Here we follow the guidelines for evaluating and expressing uncertainty provided in NIST TN 1297 [4], which are similar to the guidelines provided by the ISO Guide [5]. In general, if a measurement quantity, y, is a function of variables x_i,

$$y = f(x_1, x_2, ..., x_n) \tag{36}$$

its first-order Taylor series approximation is,

$$dy = \sum_i \frac{\partial y}{\partial x_i} dx_i \tag{37}$$

Thus, the propagation of uncertainty yields

$$u_c^2(y) = \left[\sum_{i=1}^{n}\left(\frac{\partial y}{\partial x_i}\right)u(x_i)\right]^2 = \sum_{i=1}^{n}\left(\frac{\partial y}{\partial x_i}\right)^2 u^2(x_i) + 2\sum_{i=1}^{n-1}\left(\frac{\partial y}{\partial x_i}\right)\sum_{j=i+1}^{n}\left(\frac{\partial y}{\partial x_j}\right) r_{ij}u(x_i)u(x_j) \quad (38)$$

where $u_c(y)$ is the combined standard uncertainty of the measurement result y, $u(x_i)$ is the standard uncertainty of the variable x_i, the partial derivatives $\partial y / \partial x_i$ are the dimensional sensitivity coefficients of x_i on y, and r_{ij} is the cross correlation coefficient between variables x_i and x_j. An alternative form of (38), which expresses the uncertainty propagation in a dimensionless form, is shown below and it is often more useful.

$$u_y^2 = \sum_{i=1}^{n} c_{x_i,y}^2 u_{x_i}^2 + 2\sum_{i=1}^{n-1} c_{x_i,y}\sum_{j=i+1}^{n} c_{x_j,y}\, r_{ij}\, u_{x_i} u_{x_j} \quad (39)$$

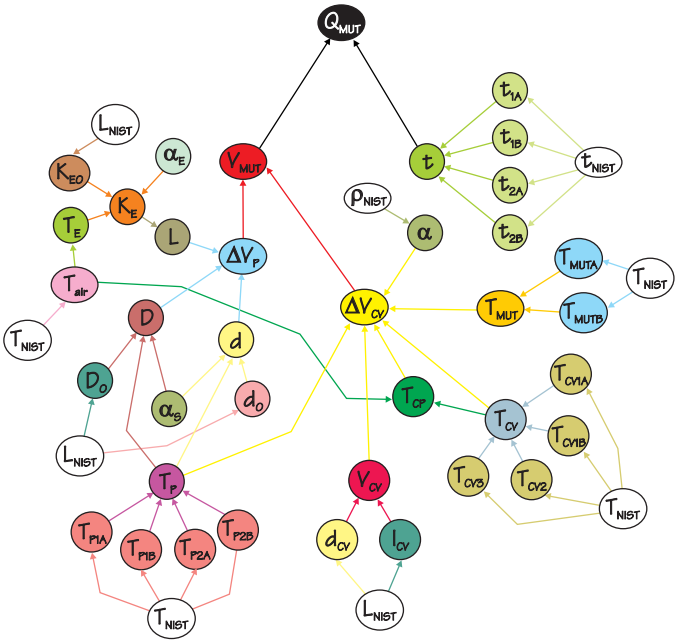

Figure 7. Graphic representation of the uncertainty analysis.

In (39), $u_y = u_c(y)/y$ is the combined dimensionless standard uncertainty of the measurement result y, $c_{x_i,y} = (\partial y / \partial x_i)x_i / y$ are the dimensionless sensitivity coefficients of x_i on y, and $u_{x_i} = u(x_i)/x_i$ is the dimensionless uncertainty of the variable x_i. Equation (39) is used here to estimate the combined uncertainty of the measurement. In many cases, the uncertainty of x_i could not be measured directly. For those cases, the same uncertainty propagation given by (39) is used for a sub-measurement process to estimate the combined uncertainty of the sub-measurement. This process is propagated throughout all the measurement components needed until the desired measured quantities are obtained.

MEASURED QUANTITIES AND THEIR UNCERTAINTIES

The uncertainty propagation can be calculated based on (15), but it is worth remembering that the flow rate in (15) is not directly measured. To obtain the uncertainty of this result, its relationship to other measured quantities is required.

According to [4], the sources of uncertainty used in assessing the combined standard uncertainty of the measurement process can be classified according to two types: *Type A* - those which are evaluated by statistical methods, and *Type B* - those which are evaluated by other means. Following this convention, each measured quantity has been classified accordingly as a u_A or u_B.

The piston prover volume, ΔV_P, can be calibrated by: (a) water draw method, (b) using a master flow meter, or (c) by using the dimensions of its diameter and the piston traveled distance. Here, the diameter/traveled-distance method is used to determine the prover volume. In mathematical terms that is,

$$\Delta V_P = \frac{\pi\left(D^2 - d^2\right)}{4}\Delta L_E = \frac{\pi\left(D^2 - d^2\right)}{4}\frac{N_E}{K_E} \quad (40)$$

where D and d are the piston prover diameter and piston shaft diameter, respectively; ΔL_E is the encoder (or piston) displacement length, K_E is the encoder constant (in pulses/cm), and N_E is the total number of pulses produced by the encoder during the calibration stroke. In our system, the value N_E may be selected by software or by the operator, to ensure that the prover is operating at the uncertainty asserted in this analysis.

In bi-directional piston prover calibrators like ours, the piston diameter will be the same regardless of the direction of piston travel. However, the shafts that are attached to both sides of the piston may have slightly different diameters. Similarly, the linear encoders monitoring the displacement of the piston shafts may have slightly different encoder constants. Therefore, for bi-directional provers, the measurement characteristics in one direction of piston travel may be different from the other. Nonetheless, because the shaft diameter assessment process is based on the entire shaft on both sides and the times measured from both encoders are used for either direction (see time measurement below), it is expected that the uncertainty for each direction be the same.

In our system, the encoders are Mitutoyo AT2N-600. A stabilizer is built into the detector to ensure a stable signal output. The encoder detector head is trued to the glass scale

inside its housing and fixed by positioning plates. The thermal expansion of the encoders is given by,

$$L_E = L_{ER}\left(1+\alpha_E \Delta T_{ER}\right) \text{ and } K_E = K_{ER}\left(1-\alpha_E \Delta T_{ER}\right) \quad (41)$$

where L_{ER} and K_{ER} are the encoder length and encoder constant at the reference temperature, respectively; ΔT_{ER} is the temperature rise from the reference temperature, and α_E is the linear expansion coefficient of the encoder.

The diameters of the prover assembly also change with the temperature following these relations,

$$D = D_R\left(1+\alpha_S \Delta T_{DR}\right) \text{ and } d = d_R\left(1+\alpha_S \Delta T_{dR}\right) \quad (42)$$

where D_R and d_R are the reference temperature diameters of the prover and of the piston shaft, respectively, and ΔT_{DR} and ΔT_{dR} are the temperature rise with respect to their reference temperature, respectively.

The uncertainty of the temperature measurements made throughout the prover will contribute to the uncertainty of the calibrator. Our calibrator uses thermistors for all temperature measurements, with twelve of them placed at various locations along the liquid flow path. At locations deemed critical, the system has duplicate sensors to improve measurement accuracy and increase system reliability. The locations of the temperature sensors in the system are shown in Figure 2. T_{Athena} is located near the heat exchanger for temperature control; T_{1A} and T_{1B} are located at prover exit-1, and T_{2A} and T_{2B} are at prover exit-2; T_{CV1A} and T_{CV1B} are located at the exit of the four-way value, T_{CV2} and T_{CV3} are placed along the length of the connecting volume; T_{MUTA} and T_{MUTB} are immediately upstream of the MUT.

The thermistors are calibrated in an isothermal bath by comparing their response to that of a standard PRT calibrated by the NIST Thermometry Group. The four calibration coefficients and the temperature uncertainty for each thermistor are obtained using a linear regression method. The uncertainty in the reference temperature, which is 0.002 K, is also classified as a type B uncertainty for each sensor. An additional uncertainty is obtained by comparing the temperature output of the calibrated sensors with the reference temperature in the isothermal bath. The average difference is assigned as the type B uncertainty and the standard deviation of the difference is assigned as a type A uncertainty. The root-sum-square of the uncertainties from the reference sensor, data regression, and temperature test, is assigned to be the combined uncertainty of each sensor. The sensors readings have 0.041 K for u_A and 0.031 K for u_B, for a worst case scenario.

The model used for the reduction of the various temperatures in the system affects the uncertainty of the calibrator results. At initial and final conditions, the average connecting volume fluid temperature, T_{CV}, is assumed to be the average value of the five temperature readings made along the fluid path.

$$T_{CV} = \left(T_P + T_{CV1} + T_{CV2} + T_{CV3} + T_{MUT}\right)/5 \quad (43)$$

In the above equation, $T_P = \left(T_{PiA} + T_{PiB}\right)/2$ is the average prover temperature (depending on the piston travel direction, $i = 1$ or 2); $T_{CV1} = \left(T_{CV1A} + T_{CV1B}\right)/2$ is the average temperature at exit of the four way valve; and $T_{MUT} = \left(T_{MUTA} + T_{MUTB}\right)/2$ is the temperature at the MUT.

This average temperature model of finite sensors could result in an uncertainty for the average temperature. This additional uncertainty in the average temperature is given by

$$E_{max} = \text{ the maximum spatial variation of the fluid temperature} \quad (44)$$

Test data show that the maximum temperature variation among the sensor locations is within 0.1 K.

The connecting volume is modeled using the following equation:

$$V_{CV} = \pi d_{CV}^2 l_{CV} / 4 \quad (45)$$

In (45), d_{CV} is the averaged internal diameter of the connecting pipe and l_{CV} is its length. There is significant uncertainty associated with the estimation of the quantities needed to precisely compute the connecting volume: piping inside diameters, piping lengths, internal volumes of the valves and elbows, the dead volume in the prover, the extra connecting volumes associated with the piping used for different MUTs, etc. However, as shown below, the sensitivity of the connecting volume determination on the computed result for the volume flow through the MUT is considerably small. Thus, the accuracy of the connecting volume determination is not considered critical for this analysis. Furthermore, the uncertainties of the dimension changes due to temperature changes are even smaller and are neglected.

In addition to an accurate determination of prover volume, the measurement of time is important. The encoder pulses are counted using a count-down counter. The uncertainty of the pulse counter is assumed to be zero. That is, no pulse is missed by the counter. The quantization of time can cause the time measurement to be off by ± 1 time base. The random uncertainty of the time measurement is 1×10^{-6} sec, for the clock frequency of 1 MHz. The uncertainty of the time base oscillator will give additional uncertainty on time measurements. The uncertainty of the oscillators was determined to be 1 ppm for the type B and 1 ppm for the type A. The prover system uses two encoders (1 and 2), each providing two chronometries (A and B): one measuring the leading edges of the encoder pulses and the other measuring their trailing edges. That is, a total of four chronometries (1A, 1B, 2A, and 2B) are used to improve the accuracy of the measured collection time. The system has two oscillators (A

and B) and thus some clocks use a same oscillator while others use a different one. Oscillator A operates on clocks 1A and 2A and oscillator B operates on clocks 1B and 2B. The type B uncertainties of the clocks are assumed to be fully correlated between clocks operated by a same oscillator.

As indicated in (15), the thermal expansion of the fluid, and not the density itself, affects the volume flow determination. In our calibrator, the expression of fluid density as a function of temperature is determined off-line, using the NIST standard oscillating tube densitometer.

Likewise, the fluid kinematic viscosity does not directly affect the flow results in this type of calibrator. However, depending on the type of MUT, the fluid kinematic viscosity can affect the flow meter output. It has been shown that one can obtain improved flow measurement performance when calibration results are expressed in non-dimensional parameters, such as Strouhal and Roshko numbers [6]. Using these, variations in the fluid temperature, kinematic viscosity, and/or density, from those used during the calibration conditions, can be compensated for. By anticipating the use of these non-dimensional parameters, our uncertainty analysis should apply to a wide range of fluid kinematic viscosity (*i.e.,* 0.5 to 2 centistokes). These fluid viscosities were measured using capillary viscometers (Schott AVS 440), which measures the time required for an amount of fluid to flow through a capillary tube of known diameter and length.

PROPAGATION COMPONENTS OF UNCERTAINTY

Based on the uncertainty propagation equation (39), the uncertainty of the sub-measurements components needs to be assessed before the prover uncertainty can be estimated. This process is propagated throughout all the measurement components needed until the desired measured quantities are obtained. The uncertainty propagation for the volume flow rate as given in (15) is shown in Table 2.

Table 2. Volume flow rate uncertainty propagation using (15).

	mean	u_A / u_B	$\%u_A$ / $\%u_B$	c_{iQ}	$Q_i\%u_A$ / $Q_i\%u_B$
ΔV_P [cc]	1514.91	0.0006	3.9E-05	1.0000	3.9E-05
		0.0474	0.0031		0.0031
t [sec]	30.0147	1.6E-05	5.2E-05	-1.000	-5.2E-05
		2.1E-05	7.1E-05		-7.1E-05
α [1/K]	0.00097	0	0	-3.4E-05	0
		2.8E-05	2.8866		-0.0001
α_S [1/K]	1.7E-05	0	0	-1.3E-07	0
		3.4E-07	2.0000		-2.6E-07
V_{CV} [cc]	195.47	0	0	4.9E-06	0
		22.73	11.628		5.7E-05
$\Delta T_{P,MUT}$ [K]	0.040	0.001	3.241	-3.9E-05	-0.0001
		0.031	77.500		-0.0030
$\Delta T_{H,CV}$ [K]	0.040	0.057	142.97	5.0E-06	0.0007
		0	0		0
ΔT_{CP} [K]	0.020	0.049	243.14	-1.3E-07	-3.2E-05
		0	0		0
Q_M [cc/s]	50.470	0.0004	--	--	0.0007
		0.0022	--		0.0043

Table 2 shows the uncertainty propagation for a volume flow of 3.0 lpm (0.8 gpm). Using the same method, the uncertainties for other flow rates are also obtained. Table 3 shows the uncertainties for a range of flows and the worst case scenario for the total uncertainty propagation for these flows. These worst case scenario values are then used for the uncertainty propagation for the calibrator:

$$u_A = 0.0019\% \text{ and } u_B = 0.0043\% \tag{46}$$

Table 3. Propagation of uncertainties for several flow rates.

Q	t_c	ΔV_P	ΔL	u_A	u_B
[lpm]	[s]	[cc]	[cm]	[%]	[%]
0.2	180	567	14	0.0019	0.0043
0.4	180	1134	28	0.000965	0.004339
0.8	120	1515	37.4	0.000727	0.004338
1.5	60	1515	37.4	0.000727	0.004338
3.0	30	1515	37.4	0.000727	0.004338
5.3	17.2	1515	37.4	0.000729	0.00434
Max				0.0019	0.00434

COMBINED UNCERTAINTY

In accordance with [4], the combined standard uncertainty for the measurement system, is given by $u_C = \sqrt{u_A^2 + u_B^2}$. That is:

$$u_C = \sqrt{(0.0019)^2 + (0.0043)^2}\,\% = 0.005\% \tag{47}$$

EXPANDED UNCERTAINTY

The approximate confidence level of the result given above is 68%. When a coverage factor of $k = 2$ is used to convert the combined standard uncertainty to an expanded uncertainty, with an approximate 95% level of confidence, the expanded uncertainty becomes:

$$U = \pm k\, u_C = 0.01\% \tag{48}$$

UNCERTAINTY OF MUT

The uncertainty analysis reported above is for the respective piston-cylinder and associated connecting volume for the prover of the NIST HLFC. The uncertainty analysis for the MUT results will depend on the flow meter type and the associated instruments used. As indicated above, improved flow measurement performance can be obtained by using non-dimensional parameters.

In addition to the uncertainty propagation discussed above, the uncertainty for the MUT should also include the standard deviation of the mean for replicated flow calibration results (*i.e.,* reproducibility♠) [7]. Reproducibility data is used because flow meter users need to know the short term stability (*i.e.,* repeatability♣) and hysteresis♥ of their instruments. Also of importance is the long term stability of the instrument as incurred when turned-off and turned-on, and the day to day changes expected from its performance. These types of reproducibility can be an order of magnitude larger than the unit's repeatabilities. The replicated uncertainty of the volumetric flow was ascertained from multiple calibration results obtained from a dual rotor turbine flow meter. By using this method, the Type A uncertainty of the calibration data for the meter included both contributions from the calibrator and MUT. These replicated uncertainty measurements were made over a wide range of flow, enabling the quantification of the combined flow meter and calibrator contributions.

The data in Table 4, was repeatedly taken at four flows (5.3, 2.3, 0.8, 0.4 lpm) (1.4, 0.6, 0.2, 0.1 gpm) over four different days. In each day, the flows tested are sequenced both from the low to the high and from the high to the low. These data shows both the repeatability and reproducibility of the system.

It is difficult to set a precise flow for the entire reproducibility test. The mean values that were shifted due to the small difference in flows tested were removed by subtracting the point value of predicted mean from the lineally fitted curve based on all the data for the given flow. The expanded uncertainties $k = 2$ are 0.016%, 0.016%, 0.030%, and 0.14% for the flows. These data show the total expanded uncertainty of the MUT were normally larger than the value of 0.01% of the system uncertainty given above, especially for the low flows where the dual-turbine meter has more uncertainty.

♠ Reproducibility is defined as the closeness of the agreement between the results of measurements of the same measurand carried out under changed conditions of measurement [7].

♣ Repeatability is defined as the closeness of the agreement between the results of successive measurements of the same measurand carried out under the same conditions of measurement [7].

♥ Hysteresis is defined as the closeness of the agreement between the results of measurements of the same measurand whether the value of the measurand is approached from a higher or lower values along its range (it is a form of reproducibility [7]).

Table 4. Replicated uncertainty – dual turbine meter tests.

Q	Day	# of samples	Ro	St	σ_{ST}	$\overline{\sigma}_{ST}$
[lpm]			[]	[]	[]	[%]
5.3	1	5	25542	1.743927		
	1	5	25848	1.743922		
	2	5	25507	1.744344		
	2	5	25974	1.744588		
	3	5	25641	1.744620		
	3	5	26044	1.744357		
	4	5	25622	1.743648		
	4	5	25885	1.743689		
		averaged	25758	1.744137	0.000384	0.0078
				expanded, $k = 2$		0.0156
2.3	1	5	10899	1.743881		
	1	5	11144	1.743737		
	2	5	10911	1.743027		
	2	5	11247	1.743129		
	3	5	10957	1.744143		
	3	5	11018	1.743514		
	4	5	10826	1.743632		
	4	5	11141	1.743893		
		averaged	11018	1.743619	0.000394	0.0080
				expanded, $k = 2$		0.0160
0.8	1	5	3697	1.744723		
	1	5	3731	1.743953		
	2	5	3619	1.743887		
	2	5	3627	1.743834		
	3	5	3630	1.742653		
	3	5	3640	1.743215		
	4	5	3654	1.74253		
	4	5	3801	1.743997		
		averaged	3675	1.743599	0.000736	0.0149
				expanded, $k = 2$		0.0298
0.4	1	5	1880	1.719506		
	1	5	1783	1.716736		
	2	5	1859	1.718620		
	2	5	1757	1.717408		
	3	5	1771	1.710190		
	3	5	1804	1.711813		
	4	5	1877	1.717497		
	4	5	1804	1.718327		
		averaged	1817	1.716262	0.00337	0.0695
				expanded, $k = 2$		0.1390

ACKNOWLEDGMENTS

This work was sponsored by the U.S. Department of Defense through its Calibration Coordination Group (CCG). The project number was CCG# 484 and the POC was Rey Cheesman of the Measurement Science Directorate, Naval Surface Warfare Center, Corona Division Corona, CA. Enlightening discussions with Paul Olivier and John Frederick of Flow Dynamics, Inc., Scottsdale, AZ; David Todd of the U.S. Navy Primary Standards Laboratory, San Diego, CA; Rusty Kauffman of the, U.S. Army Applied Physics Laboratory, Redstone Arsenal, Huntsville, AL; Steve Croasmun and David Madden of the U.S. Air Force Metrology and Calibration Program, Heath, OH; James Whetstone, John Wright, and Donald Ward of NIST are gratefully acknowledged. Special acknowledgement is given to John Stoup of Precision Engineering Division, NIST for his kind service in providing the NIST length standard.

REFERENCES

[1] G. E. Mattingly, "Flow Measurement Proficiency Testing," in ISA Flow Measurement, 2nd Ed., Practical Guides for Measurement and Control, Ch. 28 (Instrument Society of America, NC, 2001).

[2] J. D. Wright and G. E. Mattingly, *NIST Calibration Services for Gas Flow Meters: Piston Prover and Bell Prover Gas Flow Facilities, NIST SP 250-49* (National Institute of Standards and Technology, Gaithersburg, MD, 1998).

[3] API, *Manual of Petroleum Measurement Standards, Chapter 4.3: Proving Systems - Small Volume Provers, 1st ed.* (American Petroleum Institute, Washington, D.C., 1993).

[4] B. N. Taylor and C. E. Kuyatt, Guidelines for the Evaluating and Expressing the Uncertainty of NIST Measurement Results, *NIST TN-1297* (National Institute of Standards and Technology, Gaithersburg, MD, 1994).

[5] ISO, *Guide to the Expression of Uncertainty in Measurement* (International Organization for Standardization, Geneva, Switzerland, 1993).

[6] G. E. Mattingly, *The Characterization of a Piston Displacement-Type Flowmeter Calibration Facility and the Calibration and Use of Pulsed Output Type Flowmeters*, NIST J. of Res., **97** *5* (1992), pp. 509-531.

[7] ISO, *International Vocabulary of Basic and General Terms in Metrology, 2nd ed.,* (International Organization for Standardization, Geneva, Switzerland, 1993).